J. Fluid Mech. (1983), *vol.* 130, *pp.* 165–186
Printed in Great Britain

Evolution of two-dimensional disturbances in the Rayleigh–Bénard problem and their preferred wavenumbers

By A. V. GETLING

Institute of Nuclear Physics, M. V. Lomonosov Moscow State University, Moscow 117234, U.S.S.R.

(Received 17 January 1979 and in revised form 7 December 1982)

A nonlinear non-stationary problem of the development of two-dimensional convective motions in a plane horizontal fluid layer bounded by free surfaces and heated from below is studied. Horizontal dependences of the velocity and temperature are not assumed to be periodic or almost periodic; they have continuous wavenumber spectra and are represented by Fourier integrals. Vertical dependence of each variable is represented by several Fourier harmonics. Spectrum evolution is studied by means of the numerical integration of an initial-value problem. Initial disturbances of two qualitatively different classes are considered; viz those localized in horizontal extent within a narrow part of the layer as well as having the form of a roll set throughout a rather wide region. In both cases convective flows tend to evolve towards the arrays of well-established rolls with the same horizontal wavenumber a_p, which apparently seems to be the physically optimal (preferred) one for two-dimensional convection at given Rayleigh number R and Prandtl number P. We see no indications that the deviation of the initial roll-disturbance wavenumber from a_p must exceed some threshold value for giving rise to the flow readjustment in wavenumber. At sufficiently small P a decrease in a_p with increasing R is observed which agrees with experiments. A comparison is made of various theoretical models and various experimental circumstances, whence it is seen that the less stable the flow (i.e. the easier it can readjust), the better the preferred wavenumber manifests itself. In particular, roll flows periodic in a horizontal direction all over the infinite layer are highly stable, and when only such flows are considered, as has most often been the case, the preferred wavenumber is not revealed.

1. Introduction

Numerous experiments show that thermal convection of a constant-viscosity fluid in a plane horizontal layer heated from below, without thermocapillary effect, at not very small Prandtl numbers P and within a rather wide range of Rayleigh numbers R exceeding the critical one, R_c, settles down to a steady, nearly two-dimensional roll flow (see e.g. Krishnamurti 1970; Willis, Deardorff & Somerville 1972; Kutateladze, Kirdyashkin & Berdnikov 1974). The distribution of rolls in their horizontal widths (or in corresponding horizontal wavenumbers a) is peaked at a certain value depending not only on R and P but also on the prehistory of the flow, or, in other words, on the initial conditions (Krishnamurti 1970; Willis *et al.* 1972).

In particular, the experiments with controlled initial conditions of a special form, viz an artificially created two-dimensional roll flow with a given wavenumber a_0 (Busse & Whitehead 1971; Busse & Clever 1979), show that, when a supercritical R

does not exceed a certain value (depending on P), there exists a finite band of a_0 values at which the rolls are stable. When a_0 is outside this band, secondary disturbances grow, resulting in the flow readjusting to a new, 'more preferred', characteristic scale. The location of the stability region in the (a, R)-plane is described theoretically, rather satisfactorily, in terms of the analysis of the stability of a finite-amplitude two-dimensional roll flow periodic in a horizontal direction against infinitesimal three-dimensional disturbances (Busse 1967; Clever & Busse 1978; Busse & Clever 1979).

At the same time, in the experiments started from the usual uncontrolled, random 'noise') initial conditions, a much more narrow selection of physically optimal (preferred) wavenumbers is observed. Average values of measured wavenumbers are distributed within the stability region according to their proper laws and fill only its minor part (for comparison of experiments with the theory see figure 9 of Krishnamurti (1970), figure 5 of Berdnikov & Kirdyashkin (1979), and also figure 1 of Clever & Busse (1978) where the data by Willis *et al.* (1972) are used). Thus at given R and P various wavenumbers within the stability band seem not to be physically equivalent for convective flows *in general*, but equivalent only with respect to a special class of initial conditions: quite regular, periodic in a horizontal direction, two-dimensional rolls experimentally realizable only when induced artificially.

The experiments with random initial conditions exhibit a decrease in the preferred wavenumber with increasing R (see e.g. Koschmieder 1969; Krishnamurti 1970; Willis *et al.* 1972; Berdnikov & Kirdyashkin 1979) most pronounced at small P. As we saw, the theory of the stability of spatially periodic roll flows does not reveal such an effect. Still less definitely the question of the preferred wavenumbers is answered by numerical experiments simulating two-dimensional convection in a segment of a horizontal layer at cyclic lateral boundary conditions (Ogura 1971; Vasin & Vlasyuk 1974). In these calculations the stability band of wavenumbers is found to be very wide, almost coinciding with the region of the linear instability of undisturbed (motionless) fluid.

We shall see that the theoretical treatment is able to display the character of the preferred wavenumber variation with R and P and remove the seeming contradiction between the experiments with random initial conditions and the results of the stability analysis of two-dimensional rolls provided that primordial forcing of the considered flows to a spatial periodicity given from outside is rejected and the choice of the physically optimal regime is left to the system itself.

Unlike most previous studies, the horizontal dependences of calculated velocity and temperature are considered here to have continuous wavenumber spectra (including zero as their long-wave bound) and represented by Fourier integrals rather than series.† This enables one to describe flows spatially aperiodic and smoothly readjusting in the course of evolution. It turns out that sufficient freedom offered to the flow seem to be important for the physically optimal wavenumber to be manifested.

2. Governing equations and solution procedure

We consider an infinite, plane horizontal layer $0 \leqslant z \leqslant d$ of an incompressible fluid with thermal expansion (the z-axis of a Cartesian coordinate system (x, y, z) is directed

† Although the numerical analysis requires the introduction of a discrete wavenumber grid, the grid values are only *computational* parameters: when the initial conditions are fixed, then, provided the grid increment is sufficiently small, the results do not depend on its value, hence on the positions of grid points. And as Fourier series are used (as e.g. in Foster 1969; Gertsenshteĭn *et al.* 1981), by varying the wavenumbers of basic harmonics we vary automatically the initial conditions, these wavenumbers thus being in fact *physical* parameters.

vertically downwards). The hydrodynamic equations for finite disturbances of variables in the Boussinesq approximation are

$$\frac{\partial \boldsymbol{v}}{\partial t} = \boldsymbol{v} \times (\boldsymbol{\nabla} \times \boldsymbol{v}) - \boldsymbol{\nabla}\left(\frac{p'}{\rho_0} + \frac{v^2}{2}\right) - \boldsymbol{g}\alpha T' + \nu \boldsymbol{\nabla}^2 \boldsymbol{v}, \tag{1}$$

$$\frac{\partial T'}{\partial t} + \beta v_z + \boldsymbol{v} \cdot \boldsymbol{\nabla} T' = \chi \boldsymbol{\nabla}^2 T', \tag{2}$$

$$\boldsymbol{\nabla} \cdot \boldsymbol{v} = 0. \tag{3}$$

Here $\boldsymbol{v} = \{v_x, v_y, v_z\}$ is the velocity vector, T is the temperature, p is the pressure, ρ is the density, $\boldsymbol{g} = \{0, 0, g\}$ is the acceleration due to gravity, ν is the kinematic viscosity, χ is the thermal diffusivity, $\alpha = -(1/\rho)\,\mathrm{d}\rho/\mathrm{d}T$ is the coefficient of volume thermal expansion, $\beta = \mathrm{d}T_0/\mathrm{d}z$ is the unperturbed temperature gradient. The subscript 0 indicates unperturbed values of variables and the primes indicate perturbations (the primes by $\boldsymbol{v}$ are omitted since we assume $\boldsymbol{v}_0 \equiv 0$). Supposing both the layer boundaries to be undeformable, free (so that tangential stresses vanish at them), and isothermal, we write the boundary conditions at $z = 0, d$ as follows:

$$v_z = 0, \quad \frac{\partial v_x}{\partial z} = \frac{\partial v_y}{\partial z} = 0, \quad T' = 0. \tag{4}$$

We consider two-dimensional flows, putting $v_y = 0$, $\partial/\partial y = 0$. Introducing non-dimensional coordinates $\xi = x/d$, $\zeta = z/d$ and using (3), we define the stream function ψ by the equations

$$v_x = -\frac{\partial \psi}{\partial \zeta}, \quad v_z = \frac{\partial \psi}{\partial \xi}. \tag{5}$$

Now we write down the Fourier representation of the variables as

$$\psi = \frac{\nu}{d} \sum_{n=-\infty}^{+\infty} \int_{-\infty}^{+\infty} V_{a,n}\, \mathrm{e}^{\mathrm{i}(n\pi\zeta + a\xi)}\, \mathrm{d}a, \tag{6}$$

$$T' = \beta d \sum_{n=-\infty}^{+\infty} \int_{-\infty}^{+\infty} T_{a,n}\, \mathrm{e}^{\mathrm{i}(n\pi\zeta + a\xi)}\, \mathrm{d}a \tag{7}$$

(n runs through all integer values; hereinafter we shall omit commas in the subscripts on V and T whenever this cannot provoke misunderstanding). Here V_{an} and T_{an} are dimensionless and ν/d and βd are the units of velocity and temperature respectively. Since ψ and T' are real and must satisfy the conditions (4), we require

$$\left.\begin{aligned} V_{-a,n} &= -V_{an}^*, \quad V_{a,-n} = -V_{an}, \\ T_{-a,n} &= -T_{an}^*, \quad T_{a,-n} = -T_{an} \end{aligned}\right\} \tag{8}$$

(the asterisk denotes complex conjugation). Thus ψ and the original variables of the problem are expressed in terms of the spectral functions V_{an} and T_{an} as follows:

$$\psi = \frac{\nu}{d} \sum_{n=1}^{\infty} \psi_n \sin n\pi\zeta, \quad T' = \beta d \sum_{n=1}^{\infty} T'_n \sin n\pi\zeta, \tag{9}$$

$$v_x = -\frac{\nu}{d} \sum_{n=1}^{\infty} n\pi\psi_n \cos n\pi\zeta, \quad v_z = \frac{\nu}{d} \sum_{n=1}^{\infty} \frac{\mathrm{d}\psi_n}{\mathrm{d}\xi} \sin n\pi\zeta, \tag{10}$$

where

$$\psi_n = -4\int_0^\infty (\mathrm{Re}\, V_{an} \sin a\xi + \mathrm{Im}\, V_{an} \cos a\xi)\, \mathrm{d}a, \tag{11}$$

$$T'_n = -4\int_0^\infty (\mathrm{Re}\, T_{an} \sin a\xi + \mathrm{Im}\, T_{an} \cos a\xi)\, \mathrm{d}a. \tag{12}$$

Taking the curl of (1) and passing from this equation and (2) to their Fourier transforms, we obtain the following set of equations for V_{an}, T_{an}:†

$$\kappa_{an}\frac{\mathrm{d}V_{an}}{\mathrm{d}\tau} = -\kappa_{an}^2 V_{an} + ia\frac{R}{P}T_{an} + \sum_{n'=-\infty}^{+\infty}\int_{-\infty}^{+\infty}(an'-a'n)\,\pi\kappa_{a'n'}V_{a-a',n-n'}V_{a'n'}\mathrm{d}a' \tag{13}$$

$$\frac{\mathrm{d}T_{an}}{\mathrm{d}\tau} = -ia V_{an} - \kappa_{an}\frac{1}{P}T_{an} + \sum_{n'=-\infty}^{+\infty}\int_{-\infty}^{+\infty}(an'-a'n)\,\pi\, V_{a-a',n-n'}T_{a'n'}\mathrm{d}a'. \tag{14}$$

Here $R = \alpha\beta g d^4/\nu\chi$ is the Rayleigh number, $P = \nu/\chi$ is the Prandtl number, $\tau = (\nu/d^4)t$ is non-dimensional time, and $\kappa_{an} = a^2 + n^2\pi^2$.

We regard the spectrum of the flow to be bounded in a and n, putting $V_{an} = 0$, $T_{an} = 0$ when $|a| > A$ or $|n| > N$ (A, N are the constants assumed to be spectrum bounds). Then the system (13), (14) can be solved numerically, initial conditions being given. To do this we write out separately real and imaginary parts of (13) and (14) and divide the considered range of values of $|a|$ into $2M$ segments of length $h = A/2M$. Replacing the integrals over a' by sums according to the Simpson formula we obtain a set of $4(2M+1)$ nonlinear ordinary differential equations of first order with respect to the independent variable τ for the values of the functions $\mathrm{Re}\, V_{an}$, $\mathrm{Im}\, V_{an}$, $\mathrm{Re}\, T_{an}$, $\mathrm{Im}\, T_{an}$ at the points $a = mh$ ($m = 0, 1, \ldots, 2M$, $n = 1, 2, \ldots, N$). The length of the interval of the integration with respect to a' is equal to $2A - a = (4M - m)h$; when m is odd, we use the 'half' Simpson formula at the beginning of the interval (for the first segment of length h).

We shall integrate the obtained system of equations over time by the fourth-order Runge–Kutta method with a constant step h_τ. For studying the flow evolution we shall use, as well as the spectral representation of the solution, also its coordinate representation obtained by inverse Fourier transformation according to (11), (12) carried out by the Filon method (see e.g. Hamming 1962).

In each particular case the success of the calculations depends on the happiness of the choice of the computational parameters A, N, h, h_τ. The possibility of obtaining accurate results is, in principle, always attached to some finite timespan $0 \leqslant \tau \leqslant \tau_{\max}$, at given physical parameters R and P and initial conditions, $\tau_{\max}$ being dependent on the computational parameters. The point is that in the course of the evolution the real and imaginary parts of spectral functions become of alternating sign in a, the intervals between zeros of each function decreasing. When these intervals become comparable to h, the accuracy of the approximation of the integrals in (13), (14) by Simpsonian sums begins to drop sharply. In other words, sufficiently narrow spectral peaks cannot be drawn on a fixed wavenumber grid. As a result, sawlike irregularities appear in the spectrum owing to the right-hand sides of (13) and (14) being calculated by somewhat different formulae for odd and even points $a = mh$. Because these formulae have the same order of errors, one may expect the height of 'sawteeth' to

† When the velocity field is represented in the form (6) chosen here, the expansion of v_x drops out the component with $a = 0$, $n = 0$ which corresponds to the motion of the layer as a whole in the x-direction. It is readily shown that it does not change with time and may be eliminated right from the start by choosing an appropriate frame of reference.

be of the same order as the errors in the calculated values of the function. To be sure of the results we shall not use the solutions at such values of τ, as these solutions already bear marked signs of spectrum indentation (with the only exception (see figure 7) when the sawlike irregularities appear rather early but grow slowly). A great many of the regimes considered have been calculated with various h, and it is seen that until the saw appears in the run with the lesser h this run differs little in results from the one with the greater h.

Another factor affecting the $\tau_{\max}$ value may be the growth of the error caused by cutting off higher (in n) harmonics. A run, for checking its suitability from this viewpoint, is to be compared with an analogous one differing in N by 1. If N is sufficiently large then for some time the spectrum evolution proceeds in both the runs in closely similar ways. In some regimes (see §3) spectral curves of two analogous runs ultimately approach one other, and $\tau_{\max}$ is determined by the h-value. In other regimes the discrepancy between two curves all the time increases monotonically, and after its reaching an appreciable magnitude remarkable changes happen in the run with the lesser N: the oscillations of spectral functions become irregular, the growth of the main spectrum peak decelerates, in some cases an a-shift of this peak reverses, etc. This very moment sets a limit to $\tau_{\max}$. In the run with the greater N such disturbances occur appreciably later.

Most of the evolution regimes discussed in this paper have been studied with various values of N. In few cases (at some particular initial conditions) when N was not varied, the choice of the value of N was based on the results of calculations for the same R and P but other initial conditions, $\tau_{\max}$ being determined on the basis of the appearance of the spectrum, by using the signs of the accuracy losses described above. In such cases only general evolution trends revealed with certainty at the initial stage were used for further consideration.

In each case the short-wave bound $a = A$ of the spectrum is chosen to be beyond the linear-instability band, in such a way that near this bounding point absolute values of the spectral functions always remain small. Then further widening of the spectrum range used does not affect the results practically.

The time steps h_τ are to be chosen as small as necessary for the computations to be stable. When this is achieved, it is seen from checking computations with the half-steps that the accuracy of the integration proves to be very high.

Information on the runs discussed below is summarized in tables 1 and 2. Each of these runs is recognized to be accurate enough until its own $\tau_{\max}$. Some calculations are illustrated by the spectrum diagrams for the lower harmonics ($n = 1, 2$),† families of streamlines (plotted as the contours of the stream function) and families of the temperature contours. When the spectral functions contain both real and imaginary parts, for easier visualization of the results we plot on the spectrum diagram merely the modulus of this function versus the wavenumber. In the spectrum diagrams the solutions of the nonlinear problem are presented along with that of the linearized one with the same initial conditions.

3. Convection regimes with the initial conditions of class I

We impose the initial conditions of class I in such a way that within a rather wide spectrum band overspanning the region of linear instability initial (in general, not

† Hereinafter, keeping (8) in mind, we shall deal with only non-negative values of a and positive values of n.

small) disturbances of the harmonic $n = 1$ are present. Specifically, we assume that at $\tau = 0$

$$\text{Re } V_{a1} = \begin{cases} K_V a/a_1 & (0 \leqslant a \leqslant a_1), \\ K_V & (a_1 < a \leqslant a_2), \\ K_V(a_3-a)/(a_3-a_2) & (a_2 < a < a_3), \\ 0 & (a_3 \leqslant a \leqslant A), \end{cases} \tag{15}$$

$$\text{Im } V_{a1} = \begin{cases} K_V & (0 \leqslant a \leqslant a_2), \\ K_V(a_3-a)/(a_3-a_2) & (a_2 < a < a_3), \\ 0 & (a_3 \leqslant a \leqslant A), \end{cases} \tag{16}$$

$$V_{an} = 0 \qquad (n > 1), \tag{17}$$

and similarly for T_{an} (with K_T substituted for K_V); here K_V, K_T, a_1, a_2, a_3 are constants. In spectrum diagrams such initial disturbances are represented by trapezia. In physical space they are localized in ξ within a rather narrow domain of the layer; their spatial distributions constructed according to (9), (11), (12) are shown in figures 2(*a*), 5(*a*), 8(*a*). The values of all the physical and computational parameters for this series of calculations are listed in table 1.

We begin analysing the results with a slightly supercritical case. In run 1 $R = 660 = 1.004R_c$ (under the boundary conditions chosen $R_c = 657.5$). The calculated spectrum evolution is shown in figure 1, where $|V_{a1}|$ is presented ($|T_{a1}|$ has a similar form: since $\tau \approx 0.1$, $|T_{a1}| \approx 0.15\,|V_{a1}|$). The values of $|V_{an}|$ and $|T_{an}|$ with $n > 1$ all the time remain very small.

After a transient process with rapid changes in the spectrum only a narrow peak of the spectral function of the first harmonic ($n = 1$) survives. Subsequently this peak narrows and, since $\tau \approx 4$, grows showing an apparent tendency towards resembling the δ-function. This run was terminated at $\tau = 12.0$ in order to save computer time.

The spatial distributions of the disturbances at $\tau = 0$ and $\tau = 12.0$ are shown in figure 2. It is seen from such distributions for various time instants (not presented here) that convective roll motions, having primarily arisen in the region of most vigorous initial disturbances (near $\xi = 0$), then propagate further and further over the layer in both ξ-axis directions, involving a wider and wider region. The disturbances in the older rolls tend to steady values. By the end of the run they change almost not at all.

Also the values of the roll width Δ settle, this quantity being defined as the distance between two successive zeros of the function ψ on the line $\zeta = \frac{1}{2}$ in the (ξ, ζ)-plane. It is seen as an apparent tendency for the flow to evolve towards a regular periodicity in ξ; thus in the limit of $\tau \to \infty$ all the rolls would have the same Δ-value. We shall characterize this final state by the 'calculated preferred wavenumber' $a_p = \pi/\Delta$ (for the present, we define a_p for each particular run and put over the discussion of the question as to how general is the significance of such an a_p to §5).

At $\tau = 12.0$ all the well-established rolls have very similar values of Δ yielding $a_p = 2.224 \pm 0.001$ extremely close to the critical wavenumber $a_c = 2.221$ (so high precision of the evaluation of a_p is due to the structure of the solution obtained but is not the precision of the method itself).

In the linearized problem, at the same moments, the amplitudes of the disturbances being greater, the motions involve a region of considerably less horizontal extent.

Run no.	R	P	K_V	K_T	a_1	a_2	a_3	A	$2M$	N	h_τ	$\tau_{\max}$	a_p	Figure no. Spectrum	Figure no. Spatial distribution
1	660	1	0.05	0.05	$\frac{5}{4}$	$\frac{15}{4}$	$\frac{19}{4}$	5	40	3	10^{-2}	12.0†	2.22	1	2
2	10^3	0.1	0.05	0.05	$\frac{5}{4}$	5	$\frac{43}{8}$	5.5	44	3	10^{-3}	1.0	1.7	3	—
3	10^3	0.1	0.05	0.05	$\frac{5}{4}$	5	$\frac{43}{8}$	5.5	44	4	10^{-3}	1.0†	1.6	3‖	5(b)
4	10^3	0.1	0.5	0.05	$\frac{5}{4}$	5	$\frac{43}{8}$	5.5	44	3	10^{-3}	1.0	1.7	—	—
5	10^3	1	0.05	0.05	$\frac{5}{4}$	5	$\frac{43}{8}$	5.5	44	3	10^{-2}	1.8	2.24–2.26	—	—
6	10^3	10	0.05	0.05	$\frac{5}{4}$	5	$\frac{43}{8}$	5.5	44	4	10^{-2}	6.0	2.2	4	5(c)
7	10^3	10	0.005	0.05	$\frac{5}{4}$	5	$\frac{43}{8}$	5.5	44	3	10^{-2}	1.0†	—	—	—
8	3×10^3	0.1	0.05	0.05	$\frac{1}{2}$	6	$\frac{13}{2}$	7	56	4	10^{-3}	0.27	1.1–1.2	6‖	—
9	3×10^3	0.1	0.05	0.05	$\frac{1}{2}$	6	$\frac{13}{2}$	7	56	5	$\frac{2}{3}\times10^{-3}$	0.2667	1.2–1.3	6	8(b)
10	3×10^3	1	0.05	0.05	$\frac{1}{2}$	6	$\frac{13}{2}$	7	112	4	10^{-2}	0.3	2.2§	—	—
11	3×10^3	10	0.05	0.05	$\frac{1}{2}$	6	$\frac{13}{2}$	7	70	4	10^{-2}	1.2‡	—	7‖	—
12	3×10^3	10	0.05	0.05	$\frac{1}{2}$	6	$\frac{13}{2}$	7	70	5	$\frac{2}{3}\times10^{-2}$	1.2‡	2.1–2.2§	7	8(c)

† The computations could be continued to greater values of τ without marked losses in the accuracy
‡ By time $\tau = \tau_{\max}$ a slight indentation of the spectral curves was present
§ The value(s) of a_p is/are not quite accurate because of the roll flow being settled unsufficiently
‖ The figure shows only the positions of the top points of the spectral curve of $|V_{a_1}|$ at some particular time moments

TABLE 1. Summary of the runs with the initial conditions of class I

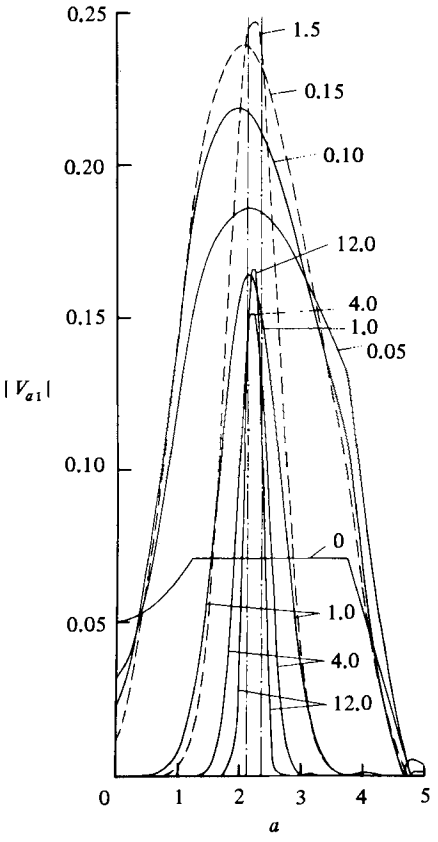

FIGURE 1. Spectral function $|V_{a1}|$ obtained in run 1 ($R = 660$, $P = 1$): ——, solution of nonlinear problem; – – –, solution of linearized problem with the same initial conditions; —·—·—, bounds of linear-instability region. Curves are labelled by τ-values.

Now we turn to moderately supercritical regimes.

Runs 2–7 correspond to the case of $R = 10^3 = 1.5R_c$ and to three different Prandtl numbers.

In figure 3 the functions $|V_{a1}|$ and $|T_{a2}|$ obtained in run 2 ($P = 0.1$) are shown. The function $|T_{a1}|$ is very similar in its form to $|V_{a1}|$. At $\tau = \tau_{max} = 1.0$ the value of $|T_{a1}|$ in its main peak is equal to 0.19. The formation of a sharp peak of $|V_{a1}|$ is observed whose position on the wavenumber axis exhibits a clear tendency to steadying with time. On both sides of it there form collateral maxima shifting towards the main one. The function $|T_{a2}|$ shows a sharp peak at $a = 0$ that reflects the development of thermal boundary layers. The values of $|V_{a2}|$, $|V_{a3}|$ and $|T_{a3}|$ remain small all the time.

In general, if we pass successively to higher values of N in the calculations then the top point of the curve representing $|V_{a1}|$ or $|T_{a1}|$ for some moment jumps in the plane of the spectral diagram in an oscillatory manner by progressively smaller distances, tending to its limiting position. In figure 3 the positions of such a point for $|V_{a1}|$ are marked as obtained in runs 2 ($N = 3$) and 3 ($N = 4$). At $\tau = 1.0$ they correspond respectively to $a = 1.7$ and 1.6; in the limit of $N \to \infty$ the maximum of $|V_{a1}|$ is obviously confined between these two a-values.

The spectrum evolution at $P = 1$ and 10 with the same initial conditions (runs 5

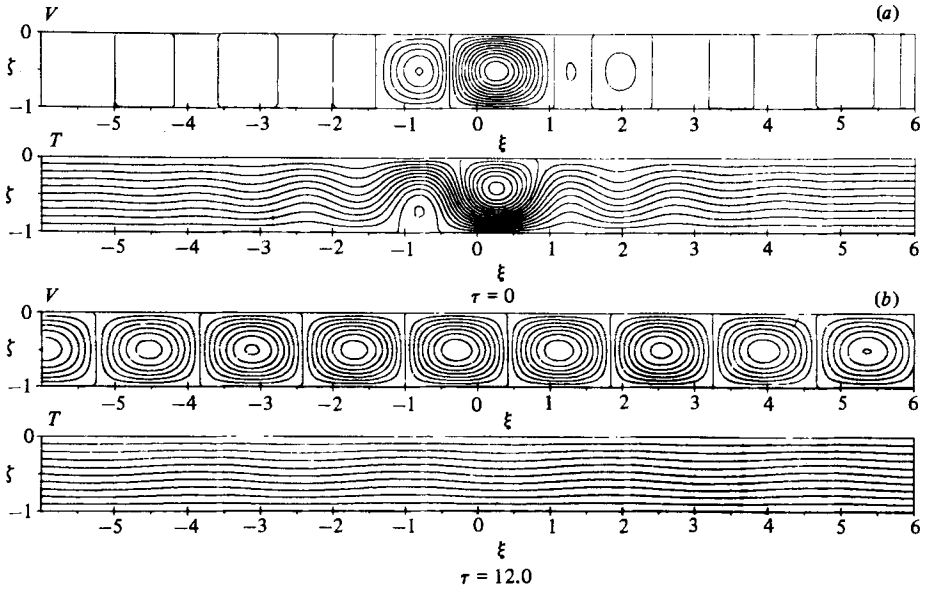

FIGURE 2. Spatial distribution of velocity and temperature in run 1 ($R = 660$, $P = 1$). Increment of contour levels of T: 0.1. (*a*) Initial disturbances (of class I); increment of ψ: 0.1. (*b*) Solution for $\tau = 12.0$; increment of ψ: 0.03.

and 6 respectively) has the same qualitative features. The case of $P = 10$ is illustrated by figure 4. For these regimes good results can be obtained in calculations with $N = 3$: there is practically no discrepancy in the spectra between the runs with $N = 3$ and 4.

On comparing regimes with three different P-values, it is seen that at $P = 0.1$ the final position of the main maximum of the spectral function of the first harmonic is appreciably shifted to the left from the critical wavenumber a_c of the linear theory, while at $P = 1$ and 10 it corresponds approximately to a_c.

The spatial distributions of the velocity and temperature obtained in runs 3 and 6 for the moments $\tau = \tau_{max}$ are shown in figures 5(*b*) and (*c*) respectively. Less developed rolls being nearer to the sides of the convecting region are somewhat narrower than mature rolls in the vicinity of $\xi = 0$. As the flow evolves, the widths of new rolls increase, the sizes of the middle rolls having already become nearly constant by time $\tau = \tau_{max}$. The roll widths tend to their final value from below. Therefore the width Δ_* of the widest roll is closest to this final value, and, as the degree of flow settling in most wide rolls implies, differs little from it. Hence the quantity π/Δ_* may be reckoned as an approximate value of the calculated preferred wavenumber a_p. It is these quantities that are listed in table 1 as a_p for the regimes $R = 10^3$. Also they correspond to the maxima of the spectral functions of the first harmonic.

We see that the calculated preferred wavenumber a_p is within the range 1.6–1.7 in the case of $P = 0.1$, and is close to the critical wavenumber $a_c = 2.22$ in the cases of $P = 1$ and 10 (very slight exceeding a_c at $P = 1$).

In runs 2, 3, 5, 6 the same initial velocities were given (as expressed in terms of the chosen dimensionless variables). This initial disturbance, as compared with the velocities in well established rolls, proved to be small when $P = 0.1$, appreciable when $P = 1$ and vigorous when $P = 10$. The initial temperature disturbance is of the same order as the steady-state amplitude values in all three cases. In order to form a view

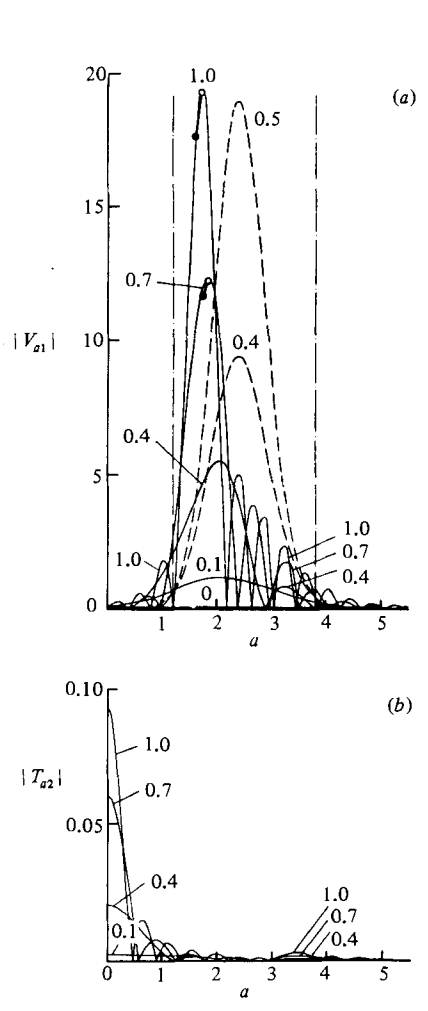

$R = 10^3, P = 0.1$

FIGURE 3

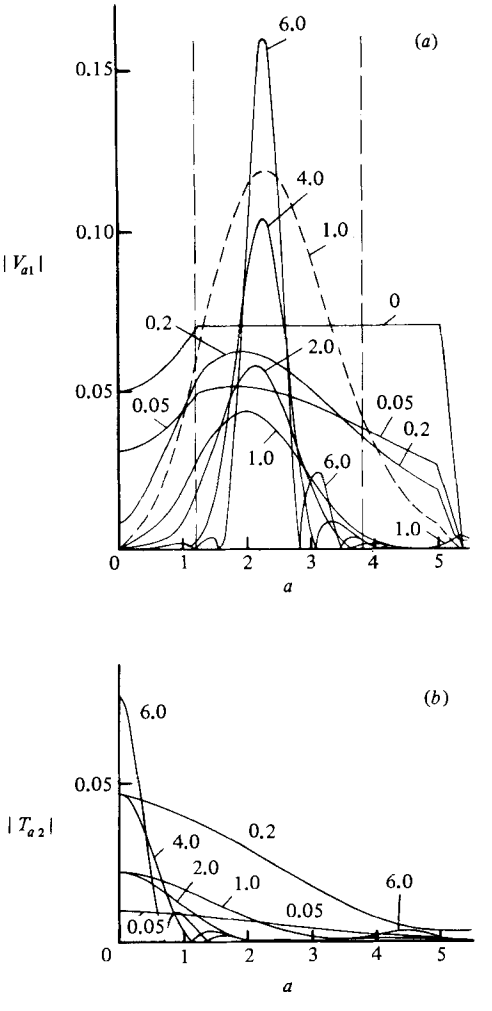

$R = 10^3, P = 10$

FIGURE 4

FIGURE 3. Spectral functions $|V_{a1}|$ and $|T_{a2}|$ obtained in run 2 ($R = 10^3$, $P = 0.1$, $N = 3$): ○, top points of spectrum curve of $|V_{a1}|$ at $\tau = 0.7$ and 1.0; ●, the same for run 3 ($N = 4$). Other notation as in figure 1.

FIGURE 4. Spectral functions $|V_{a1}|$ and $|T_{a2}|$ obtained in run 6 ($R = 10^3$, $P = 10$). Notation as in figure 1.

of an effect of the initial velocity magnitude on the process development, runs 4 and 7 were performed, which differed from runs 2 and 6 only in K_V values. In these additional runs the initial characteristic velocities were comparable to the steady-state ones. It turned out that in spite of the initial velocity being changed by a factor of 10 the process arrived at the values of the spectral functions practically the same as earlier and at the same course of temporal evolution. Differences in the spectral-function values between runs 2 and 4 became insignificant at $\tau \approx 0.6$ and between runs 6 and 7 at $\tau \approx 1$.

Now we pass on to the regimes $R = 3 \times 10^3 = 4.5R_c$ (runs 8–12). For general

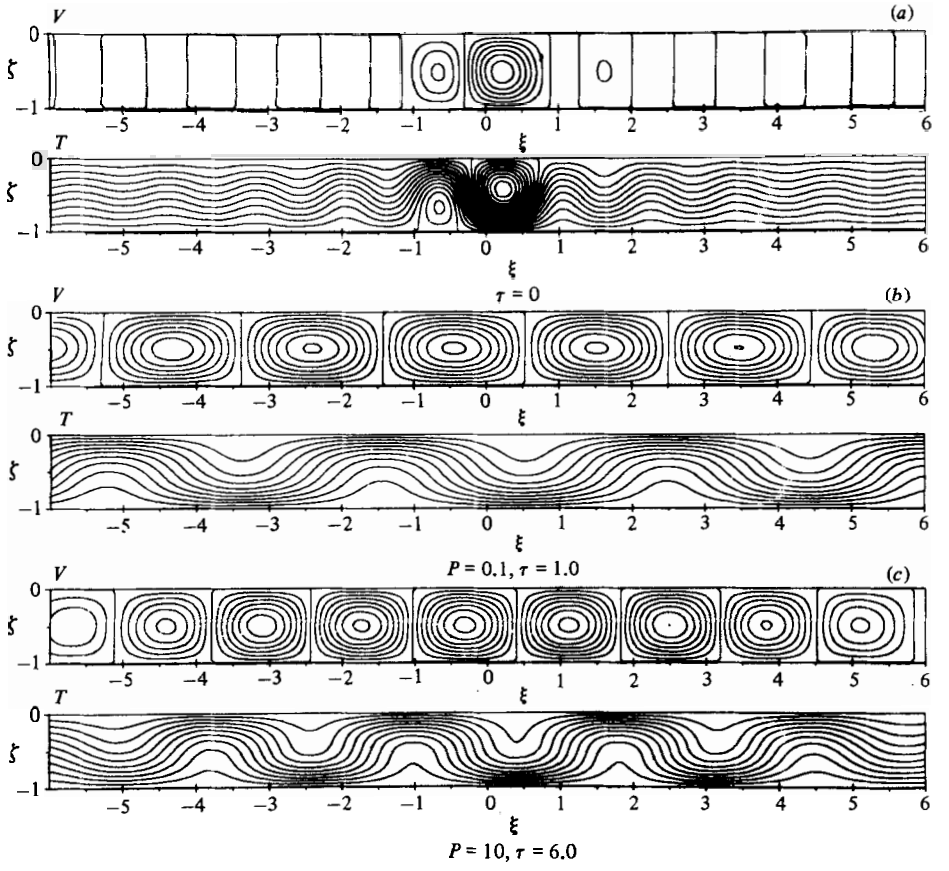

FIGURE 5. Spatial distributions of velocity and temperature in runs 3 and 6 ($R = 10^3$). Increment of T: 0.1. (*a*) Initial disturbances of class I general for runs with $R = 10^3$. Increment of ψ in runs 3 and 6: 0.2. (*b*) Solution obtained in run 3 ($P = 0.1$) for $\tau = \tau_{\max} = 1.0$; increment of ψ: 5.0. (*c*) Solution obtained in run 6 ($P = 10$) for $\tau = \tau_{\max} = 6.0$; increment of ψ: 0.05.

qualitative features the spectra evolve in the same way as when $R = 10^3$, but much more rapidly. Figures 6 and 7 show the diagrams of $|V_{a1}|$ as obtained in runs 9 and 12 ($N = 5$) respectively, for $P = 0.1$ and 10. Also the positions of the points of the spectral curves are marked for runs 8 and 11 ($N = 4$). It is interesting that the results obtained at $N = 4$ and 5 converge with time. This means that at the initial stage of the evolution higher harmonics are excited which subsequently damp and do not affect appreciably the establishment of the roll flow.

By the time $\tau_{\max}$ the most developed rolls do not attain such a degree of their settling as in the runs carried out for $R = 10^3$, especially when $P = 1$ and 10. It is seen from figures 8(*b*, *c*) that the dispersion in roll-width values is rather marked. As before, the greater the velocity in a roll the wider the roll. However, unlike the regimes at $R = 10^3$ the widths of the oldest rolls (in the middle of the convecting region) now first exceed their final values – probably owing to the impetuous growth of the disturbances at the early stage while they are yet very localized.† Subsequently the roll widths equalize. At $P = 0.1$ the total width of four middle rolls and at $P = 1$ and 10 that of three ones practically do no longer vary by $\tau = \tau_{\max}$, thus giving the

† The author is grateful to one of the referees for pointing out such a possibility.

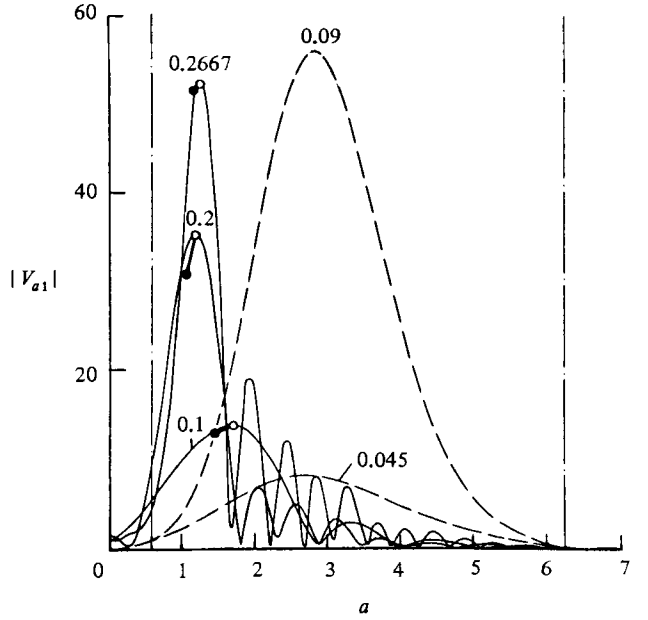

FIGURE 6. Spectral function $|V_{a1}|$ obtained in run 9 ($R = 3 \times 10^3$, $P = 0.1$, $N = 5$): ○, top points of spectrum curve at $\tau = 0.1$, 0.2, 0.2667; ●, the same for run 8 ($N = 4$). Other notation as in figure 1.

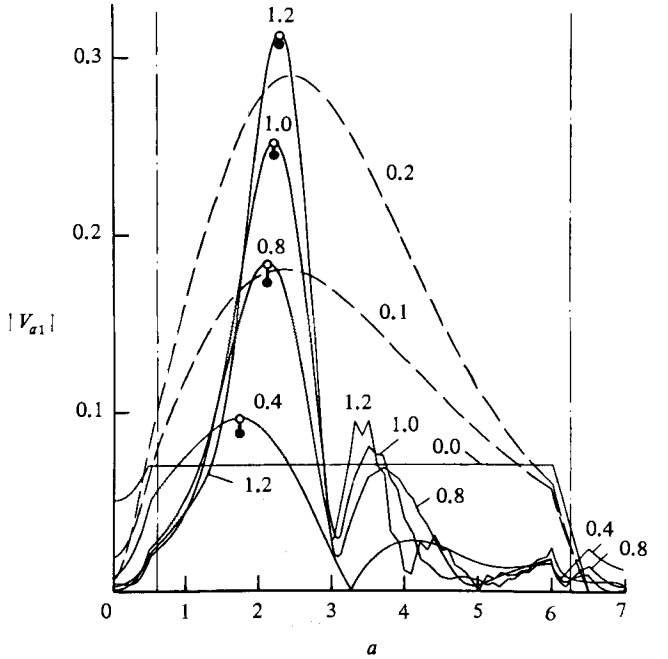

FIGURE 7. Spectral function $|V_{a1}|$ obtained in run 12 ($R = 3 \times 10^3$, $P = 10$, $N = 5$): ○, top points of spectrum curve at $\tau = 0.4$, 0.8, 1.0, 1.2; ●, the same for run 11 ($N = 4$). Other notation as in figure 1.

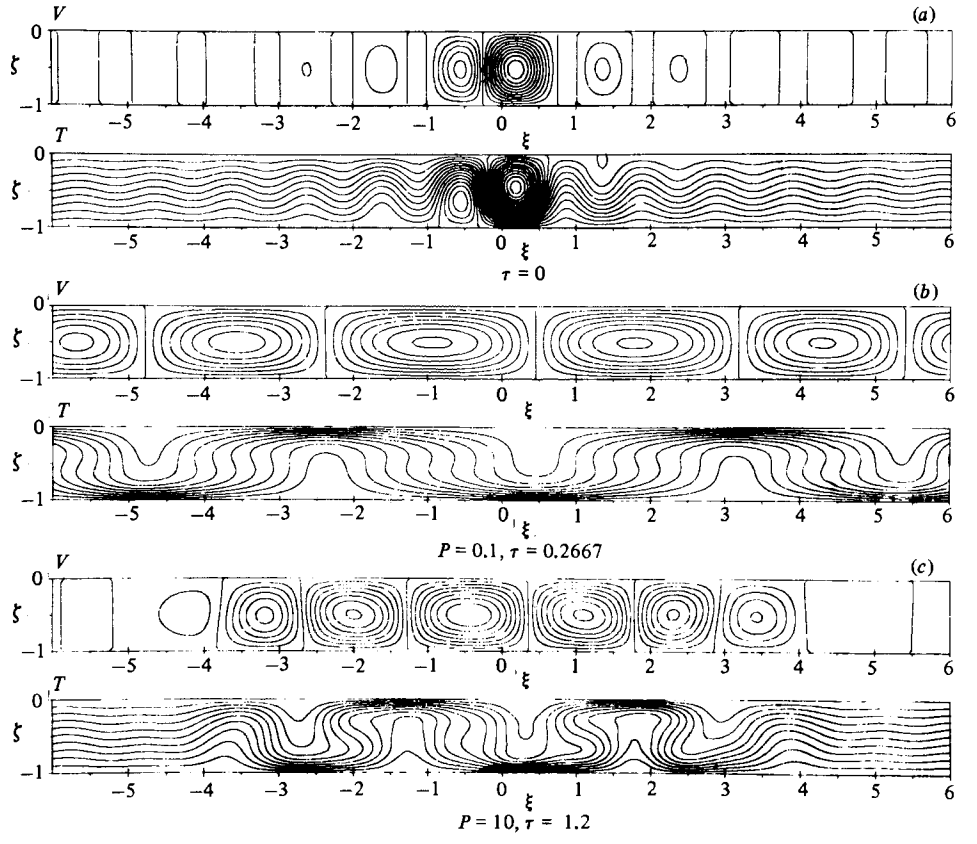

FIGURE 8. Spatial distribution of velocity and temperature in runs 9 and 12 ($R = 3 \times 10^3$). Increment of T: 0.1. (*a*) Initial disturbances of class I general for runs with $R = 3 \times 10^3$; increment of ψ: 0.15. (*b*) Solution obtained in run 9 ($P = 0.1$) for $\tau = \tau_{max} = 0.2667$; increment of ψ: 15.0. (*c*) Solution obtained in run 12 ($P = 10$) for $\tau = \tau_{max} = 1.2$; increment of ψ: 0.15.

possibility of judging the value of the calculated preferred wavenumber, although more roughly than at $R = 10^3$. This wavenumber a_p (see table 1) is within the range 1.1–1.3 at $P = 0.1$, and, as before, is close to a_c at $P = 1$ and 10.

Thus convection regimes started from the initial conditions of class I demonstrate a strong decrease in a_p with increasing R when $P = 0.1$ and do not reveal any somehow marked variation in a_p when $P = 1$ or 10.

In the regimes discussed, when $R = \text{const}$, the characteristic non-dimensional steady-state velocity U is approximately proportional to P^{-1}. For the range $10^3 \leqslant R \leqslant 3 \times 10^3$ a very crude estimate yields $U \propto R$, so that if $\beta = \text{const}$ then the dimensional velocity behaves as $\nu^{-1}\chi^0$.

4. Convection regimes with the initial conditions of class II

The initial conditions of class II are of a qualitatively different form. In most cases they were imposed as follows: at $\tau = 0$

$$V_{an} = 0 \quad (n \geqslant 1), \tag{18}$$

$$T_{a1} = -\frac{S}{4\sigma\pi^{\frac{1}{2}}}\exp\left\{-\frac{(a-a_0)^2}{\sigma^2}\right\}(\sin a_0\xi_0 + \mathrm{i}\cos a_0\xi_0), \tag{19}$$

$$T_{an} = 0 \quad (n > 1) \tag{20}$$

(S, a_0, ξ_0, σ are constants chosen appropriately). In some runs, besides, the function V_{a1} was assumed to be non-zero and given also in the Gaussian form $V_{a1} = T_{a1}$. When $\mathrm{e}^{-a_0^2/\sigma^2} \ll 1$ the spectrum (19) represents according to (12) the temperature disturbance

$$T_1' \approx S\,\mathrm{e}^{-\sigma^2\xi^2/4}\cos[a_0(\xi-\xi_0)]. \tag{21}$$

When π/a_0 is several times as small as $4/\sigma$ or smaller this disturbance resembles that produced by an array of convection rolls occupying a more or less wide (in the ξ-direction) part of the layer. The velocity field represented by the spectral function V_{a1} of the form (19) is none other than a roll flow of this kind. In our calculations (21) always held with high accuracy. The examples of the initial temperature disturbances of the form (21) are given in figures 11 (a) and 12 (a). As $\sigma \to 0$ the spectrum (19) assumes a line character:

$$\lim_{\sigma\to 0} T_{a1} = -\tfrac{1}{4}S\delta(a-a_0)(\sin a_0\xi_0 + \mathrm{i}\cos a_0\xi_0); \tag{22}$$

in physical space the disturbance becoming periodic in ξ:

$$\lim_{\sigma\to 0} T_1' = S\cos[a_0(\xi-\xi_0)]. \tag{23}$$

In all the runs discussed here $\xi_0 = 0$, so that in the case of no initial velocity $\mathrm{Im}\, V_{an} = \mathrm{Re}\, T_{an} = 0$ for any n and τ. The values of all the parameters are given in table 2.

The typical patterns of the evolution of the spectrum of the first harmonic at 'roll' initial conditions are shown in figures 9 and 10. Our attention is attracted by a pronounced drift of the main spectral peak towards smaller a when $a_0 = 2.22$ (run 13, figure 9) and towards greater a when $a_0 = 1.4$ (run 14, figure 10). In the latter case after $\tau = 0.9$ a very slow reverse drift is observed; then an almost full stop in a-drift ensues.

The character of the solution convergence with increasing N, as described in §3, holds for the initial conditions of class II. No greater N values than for class I are required, in some cases even smaller values being sufficient (cf. runs 17 and 18).

In physical space the flow evolution appears as the readjustment of the convection rolls in their width, and, at the same time, the widening of the convecting region. This is illustrated by figures 11 and 12, obtained in runs 13 and 14. A slight reverse shift of the spectral peak observed in run 14 corresponds to the roll widths equalizing, the total width of the six rolls shown in figure 12 (c) remaining practically unchanged after $\tau = 0.9$. By time $\tau = \tau_{\max} = 1.35$ the flow in this region has mainly become steady, the roll width corresponding to the wavenumber value 1.65.

Also in run 25 the sizes of the central rolls have almost settled down to a steady value by time $\tau = \tau_{\max}$.

In other runs of this series the timespans $\tau_{\max}$ were insufficient for such a settling, although the steps $h = A/2M$ were smaller than in the runs with 'localized' initial disturbances. It was impossible to evaluate the calculated preferred wavenumber a_{p}. However, the basic tendency of the flow evolution usually manifested itself in the drift of the main spectral peak. Therefore the positions a_{m} of the main maximum of the function $|V_{a1}|$ (obtained by means of square interpolation of this function) for $\tau = \tau_{\max}$ are presented in table 2 as the results of the calculations.

Run no.	R	P	a_0	σ	S	A	$2M$	N	h_τ	τ_{max}	a_m at $\tau = \tau_{max}$	Figure no. Spectrum	Figure no. Spatial distribution
13	10^3	0.1	2.22	0.4	0.355	4	64	4	0.0015	1.2	1.98	9	11
14	10^3	0.1	1.4	0.4	0.355	4	64	4	0.0015	1.35	1.68§	10	12
15	10^3	0.1	2.22	0.2	0.355	4	64	3	0.002	0.8‡	2.19	—	—
16	10^3	0.1	1.4	0.2	0.355	4	64	3	0.002	1.2‡	1.54	—	—
17	10^3	1	2.22	0.4	0.1†	5.5	44	3	0.01	1.6	2.27	—	—
18	10^3	1	2.22	0.4	0.1†	4	64	2	0.02	1.6	2.27	—	—
19	10^3	1	1.4	0.4	0.1†	4	64	2	0.02	1.6	1.76	—	—
20	10^3	1	1.8	0.3	0.6	4	64	3	0.02	1.5	1.90	—	—
21	10^3	1	2.6	0.3	0.6	4	64	3	0.02	3.0	2.55	—	—
22	10^3	10	2.8	0.3	0.6	4	64	3	0.02	10.0	2.72	—	—
23	10^3	10	1.6	0.3	0.6	4	64	3	0.02	4.0	1.68	—	—
24	3×10^3	0.1	2.22	0.3	0.355	5	80	5	0.001	0.225	2.12	—	—
25	3×10^3	0.1	0.8	0.3	0.355	5	80	5	0.001	0.25	1.10	—	—
26	3×10^3	1	1.6	0.3	0.4	6	96	4	0.01	0.35	1.68	—	—
27	3×10^3	1	2.8	0.3	0.4	6	96	4	0.01	0.4	2.8‖	—	—
28	3×10^3	10	1.4	0.3	0.6	6	96	4	0.01	1.2	1.48	—	—
29	3×10^3	10	3.0	0.3	0.6	6	96	4	0.01	2.0‡	2.99	—	—

In every run $\xi_0 = 0$

† At the initial moment a velocity disturbance $V_{a1} = T_{a1}$ is also present

‡ The computations could be continued to greater values of τ without marked losses in the accuracy

§ The maximum value of a_m ($= 1.71$) is reached at $\tau = 0.9$

‖ Although at $\tau = \tau_{max}$ $a_m \approx a_0$, the spatial distribution shows a very small widening of the rolls in comparison with time $\tau = 0$

TABLE 2. Summary of the runs with initial conditions of class II

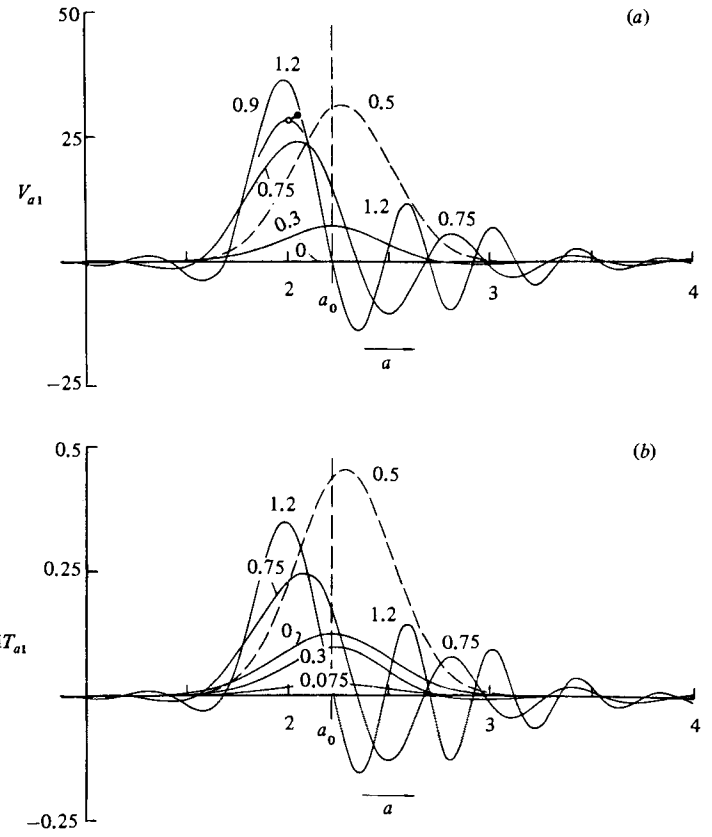

FIGURE 9. Spectral functions V_{a1} and iT_{a1} obtained in run 13 ($R = 10^3$, $P = 0.1$, $a_0 = 2.22$, $N = 4$): ○, top point of V_{a1} curve at $\tau = 0.9$; ●, the same for analogous run with $N = 5$. Vertical dashed straight line marks off position of initial wavenumber a_0. Other notation as in figure 1.

By comparing a_0 and a_m values from table 2 with a_p values from table 1 one can easily observe that the main maximum of the spectral functions of the first harmonic $|V_{a1}|$ and $|T_{a1}|$ always moves from its initial position towards a_p. When the initially imposed disturbance of the form (19) has $a_0 > a_p$ the peak drifts to the left, and when $a_0 < a_p$ it drifts to the right. In runs 14 and 25 the flow evolution looks like an asymptotic tendency of the wavenumber of convection towards the same value a_p that emerges when the flow is excited by the 'localized' initial disturbance of class I. Although in other cases τ_{max} is not great enough to draw so definite a conclusion, it is highly probable that this tendency is general, because the shift of the spectral maximum, rapid or slow, follows the described rule in any event and there is no case contradicting it. (The case of $R = 10^3$, $P = 1$, $a_0 = 2.22$ is not to be regarded as an exception because the error in the computation of a_p and a_m may be not small compared with h; moreover, a_m is not exactly the same as the wavenumber determined by the roll width.) This impression is supported by the finding that there is no case when a_m would stop changing towards a_p without reaching it (only deceleration corresponding to the asymptotic tendency $a_m \to a_p$ is observed).

Thus there are no indications that, the initial wavenumber being within some more or less wide range, the induced rolls keep this wavenumber unchanged.

A comparison between runs 13 and 15 ($a_0 = 2.22 > a_p$) and also between runs 14

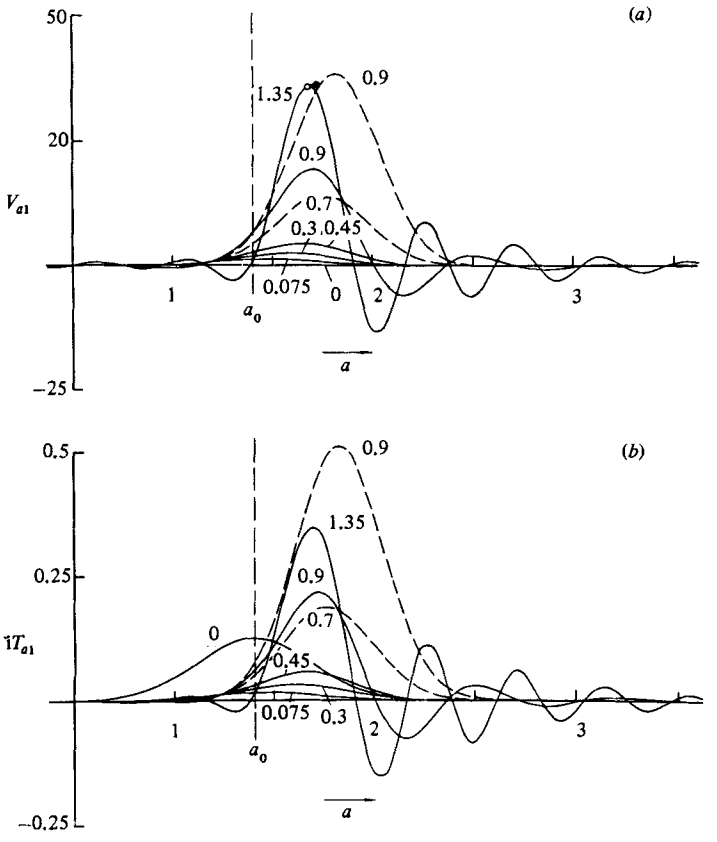

FIGURE 10. Spectral functions V_{a1} and iT_{a1} obtained in run 14 ($R = 10^3$, $P = 0.1$, $a_0 = 1.4$, $N = 4$): ○, top point of V_{a1} curve at $\tau = 1.35$; ●, the same for analogous run with $N = 3$. Vertical dashed straight line marks off position of initial wavenumber a_0. Other notation as in figure 1.

and 16 ($a_0 = 1.4 < a_p$) shows that the rate of flow readjustment depends on σ, i.e. on the width of the region involved by the initial disturbance. In both cases, at $\sigma = 0.2$ the drift of the spectral peak proceeds much more slowly than at $\sigma = 0.4$.

Besides the runs described here in detail or at least reflected in table 2, some individual tentative runs (for $R = 10^3$, $P = 0.1$ and 1) were carried out in which the initial conditions were given as a superposition of several velocity and temperature disturbances of the form (19) for $n = 1$ and 2 with different a_0 and ξ_0 and the same S. If so, the main spectral maximum developed at the point of the initial peak closest to a_p and also drifted towards a_p.

5. Summary, discussion and conclusions

The calculations carried out show that in the evolution of two-dimensional convection in an infinite horizontal layer an apparent tendency is seen towards the establishment, in the limit if $\tau \to \infty$, of the spatially periodic flow characterized by a certain wavenumber a_p. The results strongly suggest that, given R and P, the flows started from the initial conditions of both considered types tend to evolve towards one and the same a_p. The adjustment of the initially created rolls to the 'preferred' wavenumber a_p proceeds less rapidly, the wider the part of the layer occupied by these

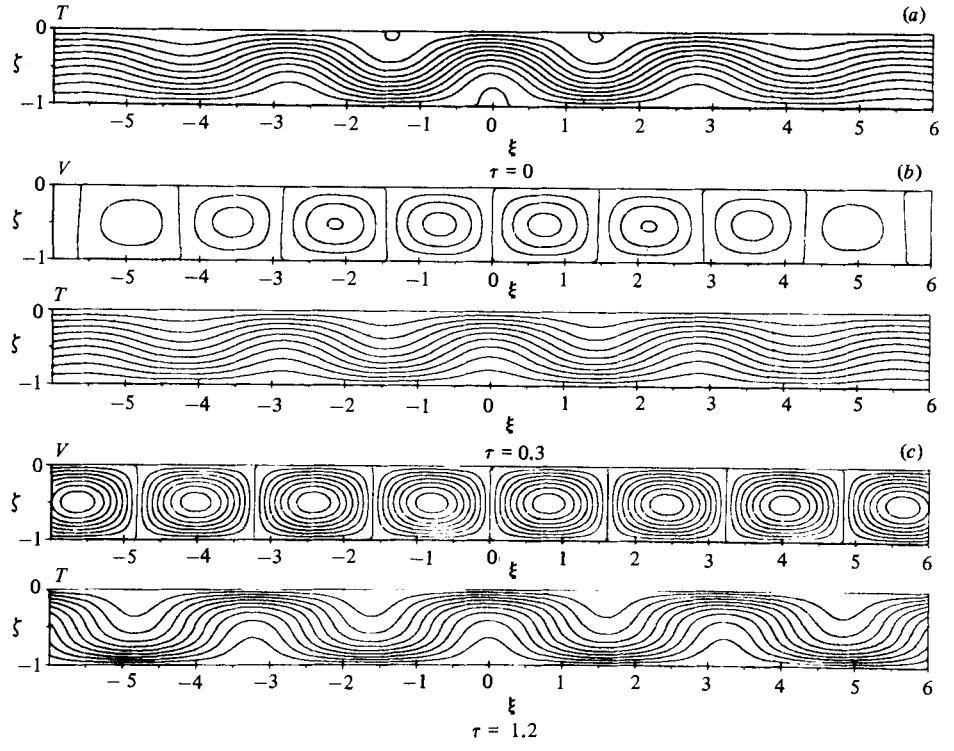

FIGURE 11. Spatial distributions of velocity and temperature in run 13 ($R = 10^3$, $P = 0.1$, $a_0 = 2.22$). Increment of ψ: 5.0; increment of T: 0.1. (*a*) Initial temperature disturbance; initial velocity = 0. (*b*) Solution for $\tau = 0.3$. (*c*) Solution for $\tau = \tau_{max} = 1.2$.

rolls. No effect of the amplitude of the initial disturbance on a_p and steady-state values of the velocity and temperature is observed. When P is sufficiently small, a_p decreases strongly with increasing R.

Our calculations with 'roll' initial disturbances do not reveal at all a rather wide spectrum band as predicted by Busse (1967), Clever & Busse (1978), Busse & Clever (1979), Ogura (1971), Vasin & Vlasyuk (1974) (and also found in the experiments with controlled initial conditions) – within that roll convective motions are stable. Although in these works P-values and/or boundary conditions differ from ours, we may, proceeding from the position of the stability regions in the (a, R)-plane found there, expect that in many of our cases the points (a_0, R) would be within the stability region or the points (a_m, R) would enter this region in the course of the drift (the region being especially extensive when the imposition of a disturbance does not break down the two-dimensional character of the flow). And, nevertheless, in all cases the rolls exhibit a tendency to readjustment to a_p. We attempt to account for this discrepancy by juxtaposing various theoretical models and conditions of various experiments and arranging them in the order of diminishing 'degree of stability' of flows, i.e. their increasing ability for readjustment. Then the tendency to distinguishing a certain preferred wavenumber will manifest itself more and more clearly.

The instabilities studied in the abovementioned works decrease the flow's characteristic scale when it is 'too large' and increase it when it is 'too small'. The tendency for a roll flow with an initial wavenumber a_0 to readjust to the preferred wavenumber a_p seems therefore to be universal. Readjusting (destabilizing) factors

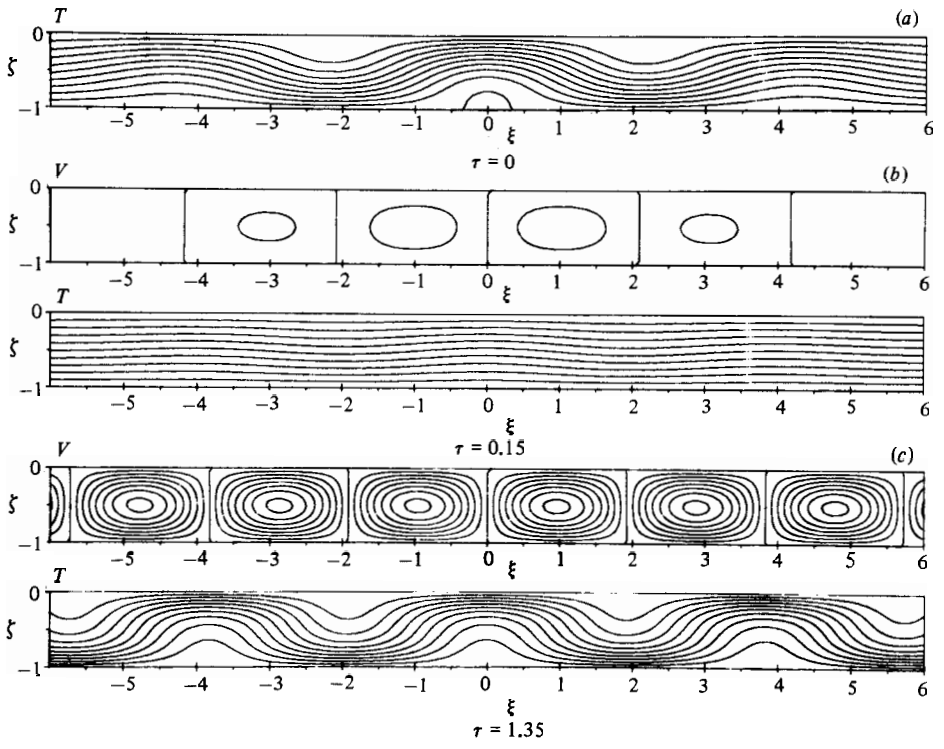

FIGURE 12. Spatial distributions of velocity and temperature in run 14 ($R = 10^3$, $P = 0.1$, $a_0 = 1.4$). Increment of T: 0.1. (*a*) Initial temperature disturbance; initial velocity = 0. (*b*) Solution for $\tau = 0.15$, increment of ψ: 2.5. (*c*) Solution for $\tau = \tau_{\max} = 1.35$, increment of ψ: 5.0.

acting more strongly for greater $|a_0 - a_p|$ may overcome the counteraction of stabilizing factors only at a finite value of $|a_0 - a_p|$. Then a finite-width wavenumber range of stable flows does exist including a_p. In other words, the instability is of threshold character.

The conditions of two-dimensional numerical models in which the flow is periodic throughout the whole infinite layer, the period being fixed by the lateral dimension of the calculation domain (Ogura 1971; Vasin & Vlasyuk 1974), ensure to such a flow very high stability. Such a flow cannot readjust smoothly in wavenumber because the rolls cannot, progressively expanding, 'move out of' the calculated domain or, contracting, 'move into' it. The width of every roll cannot be changed by the same amount other than by changing the number of the rolls in the domain. Hence the destruction or generation of some rolls, i.e. rather radical breaking of the existing flow, is necessary. The instability threshold proves to be high, the width of the wavenumber band of stable flows being very wide. In this case stability is also favoured by the fact that the number of rolls in a given spatial period is always an even integer, hence variations in wavenumber may not be arbitrary, being quantized.

The flows studied by Busse (1967), Clever & Busse (1978) and Busse & Clever (1979) retain their two-dimensional character after the imposition of a disturbance only if the latter is represented by the Eckhaus mode. In this case the flow readjustment to a new roll width all over the layer is still not realizable by means of smooth gradual expansion or contraction of the rolls, because this requires them to move by infinite distances, the generation or destruction of rolls seeming to be necessary. The

wavenumber band of stable flows is, as before, very wide.† But taking into consideration other modes that make the flow three-dimensional results in a considerable restriction of the stability band because possibilities arise for the flow's characteristic scale to change without radical breaking of the flow (of course, within certain limits), the threshold character of the instability being nevertheless retained. Because these modes are more 'dangerous' than the Eckhaus mode, their growth is considered to be the basic mechanism for flow-scale changing (Lipps & Somerville 1971; Busse & Whitehead 1971; Clever & Busse 1978; Busse & Clever 1979).

In the experiments with controlled initial conditions (Busse & Whitehead 1971; Busse & Clever 1979) the sidewalls of the tank probably play nearly the same stabilizing role as the boundaries of the calculation domain in the above numerical models. On the other hand the development of three-dimensional disturbances is not forbidden. A good agreement of the experimental results with the calculations by Busse (1967) and Busse & Clever (1979) confirms that with respect to stability this case is similar to that studied theoretically in these two papers. (More precisely, as the theoretical results by Cross *et al.* (1980) suggest, rigid sidewalls stabilize the flow somewhat less than spatial periodicity does, because boundary layers near these walls can accommodate to the flows with various wavenumbers arising in the bulk of fluid in the container.)

It is because of the presence of the wavenumber threshold for the roll instability that one can easily account for the experimentally observed hysteresis in the behaviour of the mean roll width as Rayleigh number is varied; the (uncontrolled) roll set established at some R fixing by itself the initial conditions for the process at somewhat different R (Krishnamurti 1970; Willis *et al.* 1972).

When the regimes with various R-values are realized independently, each particular experiment being started from random non-ordered initial disturbances, the tendency for a certain preferred wavenumber to be distinguished is found to be more explicit. Probably, at the initial stage the flow is weakly stable (i.e. highly changeable) owing to its disorder. The convection cells surviving among various competing ones tend to adjust to the optimal scale and optimal planform (under the simplest conditions, the roll planform). Later their stability increases, and finally in an intricated system of not-quite-regular rolls confined in a bounded region (let us recall the stabilizing role of lateral boundaries!) an equilibrium state sets in. It is characterized by the predominance of rolls of the preferred width – still there exists a considerable dispersion in the width values.

The initial conditions of classes II and I considered here are certain approximations for two limiting cases: the case of a strictly periodic roll disturbance involving the whole infinite layer (the δ-function in the spectrum) and the case of a concentrated initial disturbance (the δ-function in physical space).

The first limiting case, as we saw, corresponds to the conditions of higher stability. But the transition in the spectrum from the δ-function to the Gaussian function (initial conditions of class II) leads to considerable changes in the stability properties of the flow. As the accuracy of our calculations permits us to judge, the removal of the requirement of spatial periodicity and passage to the consideration of roll flows originally involving a finite part of the infinite layer results in the instability losing its threshold character: the flow evolves to a certain preferred wavenumber even if the initial wavenumber differs little from it. It should be noted that this is revealed

† High stability of two-dimensional spatially periodic flows with respect to disturbances of the same form (even comparable in amplitude with the initial flow) is seen also from the calculations by Gertsenshteĭn *et al.* (1981).

within the framework of a two-dimensional model although two-dimensional processes are not usually considered to be of great significance for flow-scale changing. Spatial periodicity or the presence of sidewalls prove to be more restrictive (stabilizing) conditions for such a readjustment than two-dimensionality. This is confirmed also by the fact that, the wider the region occupied by rolls (the lower σ in (19)), the less rapidly the readjustment proceeds, and the more the preferred wavenumber is masked; in the limit of $\sigma \to 0$ we are then led to a spatially periodic model with its proper wide stability range. Therefore the growth of new rolls and the widening of the convecting region can at a certain stage of the evolution make further readjustment very slow.

In contrast, one can obtain initial conditions similar to that of class I by taking σ to be very large. At such localized initial disturbances convection rolls reach the same optimal width sooner. It seems that if there are few rolls at the initial stage they 'hinder one another' less in readjusting to the optimal size.

Finally, in the limiting case of a concentrated initial disturbance one might expect the rolls to be formed whose width would correspond to the preferred wavenumber from the very beginning.

All this provides good reasons to believe that for convection in a horizontal layer there exists a physically optimal wavenumber defined uniquely (at least for flows of the type of two-dimensional rolls) which is a function of the Rayleigh and Prandtl numbers. At the same time, for the flow arriving at the roll pattern exactly corresponding to the unique wavenumber, sufficient freedom must be offered to the flow.

It is of interest that at $P = 0.1$ the calculated preferred wavenumber a_p decreases with increasing Rayleigh number and departs more and more from the value of a corresponding to the maximum growth rate of the linear theory, this value, in contrast, increasing with R. This resembles the behaviour of the preferred wavenumber of roll convection well known from experiments and most pronounced at small P. Other theoretical studies treated such a decrease in wavenumber as an effect of accessory factors such as the presence of sidewalls (Davis 1968; Cross *et al.* 1980) or the non-perfect nature of the heat conductivity of the slab bounding the layer top (Nield 1968; Nield's suggestion contrasts with the observations by Koschmieder 1969). The results presented here demonstrate the decrease in a_p with increasing R to be an intrinsic property of the convection mechanism in an infinite horizontal layer.

Discovering this effect within the framework of a two-dimensional model seems to be surprising. Lipps & Somerville (1971) have concluded from their numerical experiments that only three-dimensional calculations show increases in the roll width with increasing Rayleigh number; in two-dimensional calculations the opposite tendency is observed. On this basis they suggested that the convection tends to a steady two-dimensional regime through an essentially three-dimensional transient process affecting the final wavenumber. From the viewpoint of our results and the concept presented here of the stabilizing role of spatial periodicity one can give another interpretation of Lipps & Somerville's observation. As we saw, the decrease in a_p is a purely nonlinear effect. If initial disturbances are weak, for some time their development obeys the linearized equations according to which the wavenumber of the most rapidly growing mode increases with R rather than decrease. But having reached a considerable amplitude the calculated flow will not be able to reduce its wavenumber if the computational model gives it high stability. This must be just the case in the two-dimensional version of Lipps & Somerville's model.

Busse & Clever (1979) also assign to a three-dimensional process (the skewed

varicose instability) the major role in the mean wavenumber decreasing with increasing R. When the non-threshold flow readjustment is possible, this process is not necessary.

Nevertheless, the question of what wavenumbers would be preferred for three-dimensional disturbances evolving under similar conditions remains open as yet, as does the question about the factors affecting the selection of a preferred planform. Further studies are needed for these questions to be settled.

The author is grateful to V. I. Yudovich, V. D. Zimin, and all three referees for valuable remarks, to L. M. Alekseeva for helpful discussions, and to A. T. Fedorchenko, who shared his experience in using plotter subroutines.

REFERENCES

BERDNIKOV, V. S. & KIRDYASHKIN, A. G. 1979 On the spatial form of cellular convection. *Izv. Akad. Nauk SSSR, Fiz. Atmos. Okeana* **15**, 812–819.

BUSSE, F. H. 1967 On the stability of two-dimensional convection in a layer heated from below. *J. Maths & Phys.* **46**, 140–150.

BUSSE, F. H. & CLEVER, R. M. 1979 Instabilities of convection rolls in a fluid of moderate Prandtl number. *J. Fluid Mech.* **91**, 319–335.

BUSSE, F. H. & WHITEHEAD, J. A. 1971 Instabilities of convection rolls in a high Prandtl number fluid. *J. Fluid Mech.* **47**, 305–320.

CLEVER, R. M. & BUSSE, F. H. 1978 Large wavelength convection rolls in low Prandtl number fluids. *Z. angew. Math. Phys.* **29**, 711–714.

CROSS, M. C., DANIELS, P. G., HOHENBERG, P. C. & SIGGIA, E. D. 1980 Effect of distant sidewalls on wave-number selection in Rayleigh–Bénard convection. *Phys. Rev. Lett.* **45**, 898–901.

DAVIS, S. H. 1968 Convection in a box: on the dependence of preferred wavenumber upon the Rayleigh number at finite amplitude. *J. Fluid Mech.* **32**, 619–624.

FOSTER, T. D. 1969 The effect of initial conditions and lateral boundaries on convection. *J. Fluid Mech.* **37**, 81–94.

GERTSENSHTEĬN, S. YA., RODICHEV, E. B., SEMIN, V. N. & SHMIDT, V. M. 1981 On the nonlinear convective motions in 'double-diffusive' media. *Dokl. Akad. Nauk SSSR* **257**, 570–574.

HAMMING, R. W. 1962 *Numerical Methods for Scientists and Engineers.* McGraw-Hill.

KOSCHMIEDER, E. L. 1969 On the wavelength of convective motions. *J. Fluid Mech.* **35**, 527–530.

KRISHNAMURTI, R. 1970 On the transition to turbulent convection. Part 1. The transition from two- to three-dimensional flow. *J. Fluid Mech.* **42**, 295–307.

KUTATELADZE, S. S., KIRDYASHKIN, A. G. & BERDNIKOV, V. S. 1974 The velocity field in a convection cell of a horizontal fluid layer at thermal gravitational convection. *Izv. Akad. Nauk SSSR, Fiz. Atmos. Okeana* **10**, 137–145.

LIPPS, F. B. & SOMERVILLE, R. C. J. 1971 Dynamics of variable wavelength in finite-amplitude Bénard convection. *Phys. Fluids* **14**, 759–765.

NIELD, D. A. 1968 The Rayleigh–Jeffreys problem with boundary slab of finite conductivity. *J. Fluid Mech.* **32**, 393–398.

OGURA, Y. 1971 A numerical study of wavenumber selection in finite-amplitude Rayleigh convection. *J. Atmos. Sci.* **28**, 709–717.

VASIN, V. G. & VLASYUK, M. P. 1974 On the wavelengths of two-dimensional convective motions in a horizontal fluid layer heated from below. *Inst. Appl. Math. Acad. Sci. USSR, Preprint* no. 84 (in Russian).

WILLIS, G. E., DEARDORFF, J. W. & SOMERVILLE, R. C. J. 1972 Roll-diameter dependence in Rayleigh convection and its effect upon the heat flux. *J. Fluid Mech.* **54**, 351–367.